The Synchronous Oscillator: A Synchronization and Tracking Network

VASIL UZUNOGLU, MEMBER, IEEE, AND MARVIN H. WHITE, FELLOW, IEEE

Abstract—**The synchronous oscillator (SO) is a free-running oscillator which oscillates at its natural frequency in the absence of an externally applied signal. In the presence of a signal, the oscillator synchronizes with and tracks the input waveform with an acquisition time inversely proportional to the tracking bandwidth. The SO possesses a constant output signal amplitude in the tracking region and an adaptive tracking bandwidth proportional to the input signal level. In operation, a decrease in the input carrier-to-noise ratio reduces the SO's tracking bandwidth to maintain a constant carrier-to-noise ratio at the SO's output. An SO can track signals which have very low carrier-to-noise ratio. For example, a 70-MHz SO can perform phase acquisition in less than 400 ns and track a 140-MHz carrier with an input carrier-to-noise ratio of −40 dB (wide-band noise), while maintaining a 400-kHz tracking range. The SO has a very narrow resolution bandwidth, similar to a spectrum analyzer, which is independent of the tracking range and makes the noise rejection properties of an SO very high. Resolution bandwidth is a function of the regeneration process within the SO network, which is not found in other tracking networks. The paper presents the theory and experimental characterization of SO's in terms of selectivity, noise rejection, carrier-to-noise improvement, tracking range, and acquisition time. A specific application is described for SO carrier and clock recovery networks in a 60- and 120-Mbits/s QPSK modem with bit-error-rate (BER) performance approaching that of hard-wired connection.**

I. Introduction

SYNCHRONIZATION is an important concept in coherent digital communication systems, where both the carrier and clock must be regenerated in the receiver. The benefits of synchronization lie in the conservation of bandwidth and signal power as well as error-free identification. A synchronization network element must possess the following properties:

1) excellent filtering properties (high selectivity) for noise rejection;
2) high sensitivity to recover the signal buried in noise (low-injection signal conditions);
3) wide tracking bandwidth;
4) fast acquisition time in burst-mode operation;
5) recovered output amplitude must be independent of injection frequency and amplitude;
6) phase difference between input and output must be linear with frequency and amplitude;
7) low steady-state phase error between input and output signals;
8) low bit-error-rate (BER);
9) internal memory (storage) in absence of synchronization pulses; and
10) frequency stability with power supply and temperature variations.

In addition to the above properties, the synchronization network must be cost-effective, operate with low-power requirements, and occupy a small storage area. In this paper we will describe a synchronization network comprised of an injection-locked synchronous oscillator to achieve the above requirements for coherent digital communication systems. In addition to carrier and clock recovery applications, the synchronous oscillator (SO) possesses additional features such as frequency division, adaptive bandwidth, and operation under the injection of a signal which is harmonic of the free-running frequency of the SO. The independence of the tracking range from the resolution bandwidth enables the SO to achieve superior performance over conventional phase-locked loops.

Van der Pol [1], [2] first introduced the concept of controlling the frequency of oscillators by externally injected signals. Adler [3] analyzed an early injection-type oscillator and derived a differential equation describing the oscillator phase as a function of time, which yielded an understanding of the basic locking phenomena in terms of a simple physical model, namely, the motion of a pendulum suspended in a viscous fluid inside a rotating container. Adler's work provide the foundation for subsequent papers by Kurokawa [4], [5], Khohlow [6], Minorski [7], Hayaski [8], Dewan [9], [10], and Runge [11]. Runge introduced current injection into a VCO to increase the pull-in range of the Van der Pol oscillator [11] operating in a phase-locked loop.

The SO described in this paper is a unique free-running oscillator which oscillates at its natural frequency ω_o in the absence of an externally applied input signal ω_i [12], [14]. The latter is referred to as the injected frequency or carrier. When ω_i is applied to the SO and if it lies within the tracking range $-\Delta\omega$ of the SO (i.e., $|\omega_o - \omega_i| < \Delta\omega$), then the SO starts "tracking" the external signal. The acquisition time of the SO is several orders of magnitude faster than conventional PLL's, which are limited by the trade-off between noise rejection and acquisition time in the loop filters [15]. Once the process of acquisition (synchronization) is completed, a phase difference exists between the

Manuscript received March 11, 1985; revised July 8, 1985.
V. Uzunoglu is with Fairchild Industries, Germantown, MD 20874
M. H. White is with Lehigh University, Bethlehem, PA 18015.

0018-9200/85/1200-1214$01.00

input and output terminals of the SO. This phase offset per unit frequency is very low in a SO due to the high internal gain and wide tracking range. An important aspect of the SO is its performance as an adaptive filter, where the tracking range is proportional to the input signal amplitude. A reduction in the input carrier-to-noise ratio decreases the tracking bandwidth to maintain a constant output carrier-to-noise ratio. The main noise rejection property of a SO lies in its narrow resolution bandwidth. It is interesting to note that the resolution bandwidth is independent of the tracking range; yet both affect the noise rejection properties of a SO, the resolution bandwidth being by far the most effective one.

We will present an example of the SO in carrier and clock recovery networks with specific application to QPSK modems in order to illustrate their importance in satellite communication systems; however, the requirements of these systems fail to exercise the actual capabilities of the SO. In contrast to conventional filter approaches, the SO through its adaptive tracking bandwidth and very narrow resolution bandwidth permits the extraction of information from signals with extremely low carrier-to-noise ratios, such as -40 dB while tracking at several hundred kilohertz to permit rapid phase acquisition. This paper will describe the basic theory and experimental results obtained on injected-locked synchronous oscillators with emphasis on selectivity, noise rejection, carrier-to-noise improvement, tracking range, and phase acquisition.

II. Theory of the Synchronous Oscillator

Fig. 1 illustrates the basic injection-locked synchronous oscillator circuit and a functional description of its operation. The oscillator is a modified Colpitts oscillator with two active elements: transistor T_1 accepts the injected signal, amplifies it, and injects current into transistor T_2. Transistor T_1 is a active emitter load for transistor T_2. The dc current in both transistors is determined mainly by the bias resistor G. Transistor T_2 has three feedback paths: 1) a path thru C_1 to the base of T_2 (the value of C_1 is large and is considered a "short" at the frequency range of interest); 2) a path from the point between C_2 and C_3 to the emitter of T_2; and 3) a series negative feedback to T_2 provided by T_1. Feedbacks 1) and 2) are positive while feedback 3) is negative. The bias resistor G is adjusted so that both transistors operate in their linear-active region with equal collector-to-emitter voltage drops. L_c is an RF choke (isolation) and L, C_2, C_3 form the tank circuit. The variable resistor R_A controls the injection level and secures the isolation of the SO from the input drive circuit. The supply voltage is typically 5 V, and the power dissipation is approximately 5–10 mW.

In operation the SO is a nonlinear oscillator with high internal gain and a saturated output amplitude in the tracking range. The injected input signal only modulates the phase and does not disturb the output amplitude of the oscillator. This phase modulation is the key to SO operation. With reference to Fig. 1, the transconductance G_{m1}

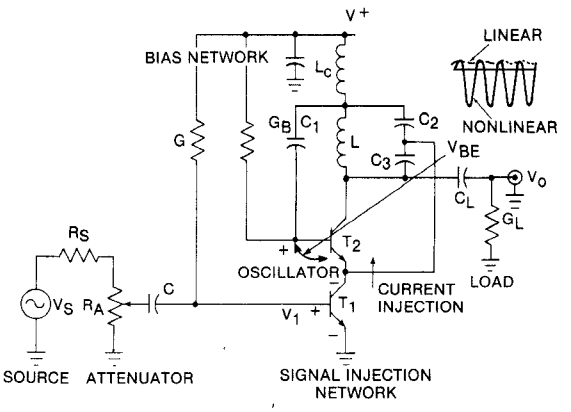

Fig. 1. Functional description of the SO circuit.

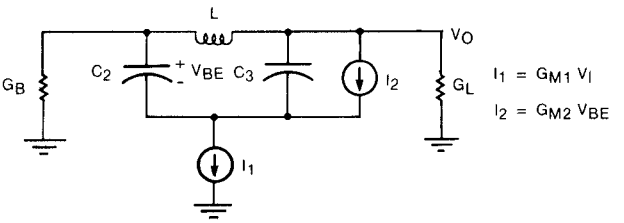

Fig. 2. Linear analysis of the SO.

of T_1 provides signal injection of current into T_2, while the transconductance G_{m2} of T_2 overcomes circuit losses. In general these transconductances are nonlinear [17]. In order to understand the concept of synchronization, we approach the SO operation with a linear analysis of the oscillator output voltage V_o, as shown in Fig. 2. A small-signal analysis of the circuit in Fig. 2 requires $G_{m2} \geq G_L C_2/C_3$ to sustain circuit oscillations, and $G_L \gg G_B$ yields

$$\omega_o^2 = \frac{C_2 + C_3}{LC_2C_3} \tag{1}$$

for the "free-running" oscillator frequency and

$$\ddot{V}_o + \omega_o^2 V_o = \frac{G_{m1}}{C}\dot{V}_i \tag{2}$$

for the fundamental differential equation, which describes the small-signal operation of the injection-locked synchronous oscillator subjected to an input signal voltage V_i, where $C = C_3(1 + C_3/C_2)$.

We may analyze the operation of the SO by assuming solutions of the form

$$V_o = \bar{V}_o e^{j(\omega_i t + \theta_o)} \tag{3}$$

$$V_i = \bar{V}_i e^{j(\omega_i t + \theta_i)} \tag{4}$$

and defining

$$\phi = \theta_o(t) - \theta_i \tag{5}$$

as the instantaneous differential phase and

$$\Delta\omega = \omega_o - \omega_i \tag{6}$$

as the instantaneous tracking range. Substituting (3)–(6)

into (2) yields the transformed equation

$$\dot{\phi} = -3K(\sin\phi - \Delta\omega/K) \tag{7}$$

where

$$K = \frac{G_{m1}\bar{V}_i}{2C\bar{V}_o} \tag{8}$$

is the injection constant for the synchronous oscillator.

There are two regions of operation for the SO

1) driven but unlocked $\Delta\omega/K > 1$, and
2) driven and locked $\Delta\omega/K \leqslant 1$.

The condition for synchronization or "lock-in" is given by the requirement

$$\Delta\omega/K \leqslant 1, \qquad \text{for synchronization and "lock-in"} \tag{9}$$

with the SO's tracking bandwidth

$$\Delta f_o = \frac{G_{m1}\bar{V}_i}{2C\bar{V}_o\pi} \tag{10}$$

which is an instantaneous adaptive tracking bandwidth proportional to the magnitude of the input signal $\bar{V}_i$. We may define a gain-tracking-bandwidth product as

$$\frac{\bar{V}_o}{\bar{V}_i} \times \frac{G_{m1}\bar{V}_i}{2C\bar{V}_o\pi} = \frac{G_{m1}}{2\pi C}. \tag{11}$$

In (10) $\bar{V}_o$ is a constant and with a specified bias condition (i.e., fixed G_{m1}), the tracking bandwidth will adaptively follow changes in the input signal level to preserve the relationship shown in (11).

The driven but unlocked SO may be analyzed, following the technique of Adler [3], to find a solution of (7) for ϕ

$$\tan[\phi/2] = \frac{K}{\Delta\omega} + \frac{K}{\Delta\omega}\sqrt{(\Delta\omega/K)^2 - 1} \cdot \tan\left[\frac{3K(t-t_o)}{2}\sqrt{(\Delta\omega/K)^2-1}\right] \tag{12}$$

where t_0 is an integration constant. The differential phase ϕ can be seen from (12) to be a periodic function of time and, therefore, the output voltage V_o has a discrete Fourier spectrum. The spectrum component of the SO's output voltage at the injection frequency ω_i may be found, following the method of Armand [16], as

$$\bar{V}_o(\omega_i) = \frac{j\bar{V}_i}{\frac{\Delta\omega}{K} + \sqrt{(\Delta\omega/K)^2 - 1}} e^{j\omega_i t}. \tag{13}$$

Thus, the unsynchronized but driven SO produces a discrete Fourier component at the injection frequency whose phase is $\pm\pi/2$ and changes sign with the frequency difference. We also observe the amplitude characteristics provide frequency discrimination or filtering, an important property of the SO.

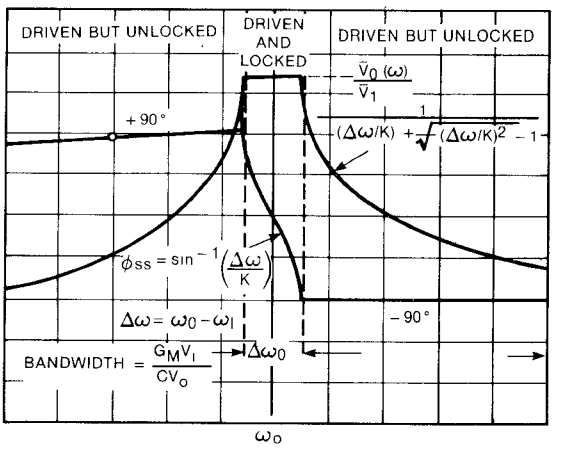

Fig 3. Transfer function (gain-phase) for the simple SO circuit

An analysis of the driven and locked SO shows that the steady-state phase error in the lock-in range becomes

$$\phi_{ss} = \sin^{-1}(\Delta\omega/K) \tag{14}$$

while the amplitude of the SO's output signal $\bar{V}_o$ is constant. An exact analysis of the SO operation in the lock-in region requires a nonlinear treatment [17]. The high internal gain of the SO maintains the output voltage constant within the lock-in range, while the input signal modulates the phase of the oscillator. Fig. 3 illustrates the amplitude and phase behavior of a SO as studied experimentally with a network analyzer with the vertical axis representing the steady-state gain $\bar{V}_o/\bar{V}_i(\omega_i)$, at the injection frequency.

We have discussed the steady-state characteristics of the SO; however, an important measurement is the phase acquisition time which is the time for the SO to reach steady-state from an unlocked condition. An analysis of (7) for the "driven and locked" region gives the time for the phase error

$$\tau(1\text{ percent}) = \frac{1}{K\sqrt{1-(\Delta\omega/K)^2}} \tag{15}$$

to settle to within 1 percent of the final steady-state value, as given by (14). The importance of the injection constant K and the offset frequency difference $\Delta\omega$ are observed in (15). Low offsets, increased signal drive, and high G_m/C ratios lead to fast phase acquisition in SO's. We observe the phase acquisition time increases in (15) as $\Delta\omega$ approaches the edge of the lock-in range and this increase is countered by the high internal gain of the SO.

An important aspect of SO operation is the response of the SO to an injection signal at harmonics of the fundamental free-running oscillator frequency ω_o. An analysis of an SO under harmonic excitation indicates the injection constant K is increased by the order of the harmonic N.[1]

[1] Insertion of $N\omega_i$ for ω_i in (4) provides an injection constant $K = NG_{m1}V_i/2CV_o$ in place of (8). An SO in the fundamental mode exhibits a $\pm 90°$ phase shift over the tracking range, while an SO operating in the nonfundamental mode with harmonic excitation N exhibits a $\pm 90°/N$ phase shift over the tracking range.

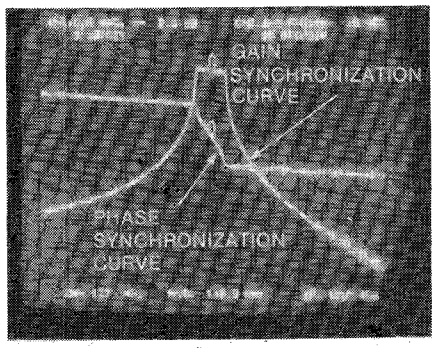

Fig. 4. Gain-phase synchronization curves of an SO.

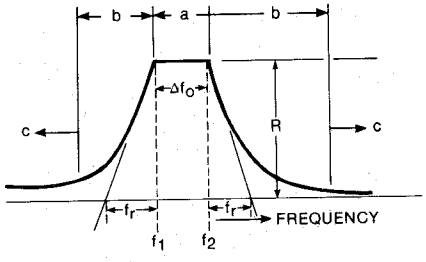

Fig. 5. Operation regions of an SO.

Thus, there is an improvement in the "tracking" bandwidth by N and the phase offset is reduced by N for small frequency offsets. In addition, the effective time constant for phase acquisition is also decreased by N for small frequency offsets. A perhaps more interesting aspect of harmonic excitation lies in the dramatic selectivity improvement in the frequency discrimination characteristics of the SO about the free-running SO frequency. The selectivity of the SO under harmonic excitation is improved by the $Q = \omega_o/\Delta\omega$ of the filter. A feature of harmonic excitation is the improved selectivity and the reduction in total phase shift across the lock-in range.

III. Experimental Results

Fig. 4 illustrates the gain-phase synchronization curves for an experimental SO. Fig. 5 illustrates the various regions of operation, which we will describe in detail. There are three distinct regions in an SO synchronization curve. Region "a" is the tracking range or the so-called driven and locked region, where the SO is synchronized to the injected carrier between the frequencies f_1 and f_2 ($\Delta f_o = f_2 - f_1$). The output amplitude is constant in this region of operation. The second region, "b", is the transition region or the so-called driven but unlocked region. This region begins as the injected carrier starts to interact with the oscillator frequency and commences when the SO is "tracking" the injected carrier frequency. The nature of this transition region varies depending upon modifications to the basic SO circuit and the manner of signal excitation. In general, the transition region is abrupt. Region "c" is characterized by the external circuit elements (i.e., pre- and post-filtering) and represents a reduced interaction between the injected carrier and the SO.

The synchronization curves of an SO have several features worthy of mention. The flatness of the gain synchronization curve is a unique property of the SO and distinguishes the latter from linear networks and, in particular, injection-type Van der Pol oscillators which are characterized by an output amplitude dependent upon the injected carrier amplitude and frequency [1], [2]. The primary function of the injected signal is to modulate the phase of the SO, while the SO's amplitude remains unchanged in the lock-in region. Outside the lock-in region, the injected signal determines the frequency discrimination or filtering characteristics of the SO, while the SO's phase remains unchanged. If the SO were a linear network, then according to linear network theory [18], [19], the phase of the transfer characteristics should display abrupt changes and extend several octaves beyond the abrupt gain changes within the transition regions. An additional feature of the SO is the almost linear phase throughout the tracking region.

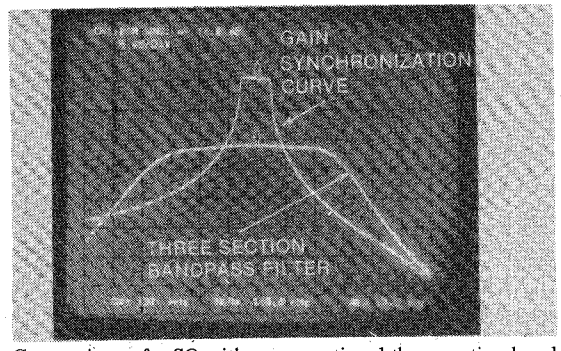

Fig. 6. Comparison of a SO with a conventional three-section bandpass filter. The SO is unmodified as shown in Fig. 1.

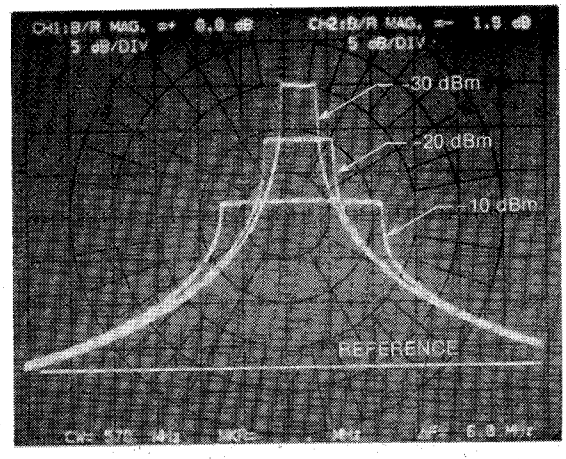

Fig. 7. Adaptive "tracking" bandwidth and "gain-attenuation" features of an SO.

The so-called "skirt" selectivity (R/f_r from Fig. 5) of a simple SO (unmodified by external networks and harmonic excitation) is considerably higher than a linear filter. Fig. 6 compares the skirt selectivity of a three-section 140-MHz bandpass filter to the filter characteristics of a simple SO operating at a center frequency of 140 MHz. The SO has a skirt selectivity of 10 dB/600 kHz compared with a three-section filter selectivity of 10 dB/2.4 MHz.

An important aspect of SO's is the adaptive "tracking" range as described in (10) and shown in Fig. 7 for injection carrier levels of -30, -20, and -10 dBm. Since the

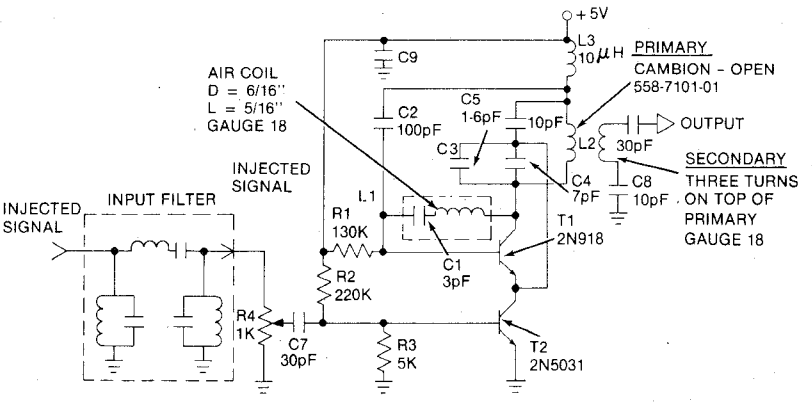

Fig. 8. Modified SO to enhance filtering performance.

output amplitude remains unchanged in the lock-in region, the network analyzer displays a different "gain" or "sensitivity"[2] characteristic for each input signal level. The −30-dBm carrier causes the highest "gain" with respect to the reference level 2, as defined in Fig. 5; however, if reference level 1 were used for the comparison, then the −30-dBm carrier would create the highest "attenuation" providing all curves are referenced to level 1. The SO features carrier selectivity, as illustrated in the decreasing bandwidth and upward swing in the curves of Fig. 7, with simultaneous improvement in noise rejection. For example, at an injection level of −100 dBm the tracking range reduces to 18 kHz. Thus, as a filter or as a tracking network, the bandwidth of a SO depends upon the injection level of the carrier. A transfer characteristic of a SO must specify the injection level. A SO is an RF filter with variable bandwidth and variable "gain-attenuation" level—a function of injected carrier amplitude—in contrast with linear filters, where gain and bandwidth are independent of injection level. Thus, the SO is an adaptive network element for signal processing.

A. Performance Enhancement Techniques

Several methods have been examined to enhance the performance of the SO's:

1) addition of a series-tuned circuit in the feedback path of the oscillator transistor;
2) addition of an external bandpass filter at the input of the SO;
3) harmonic injection into the SO;
4) combinations of 1)–3); and
5) cascaded operation of SO's.

The first four techniques are illustrated in Fig. 8 in the dotted lines. The SO of Fig. 8 oscillates at 560 MHz with the addition of the series L_1C_1 tuned circuit. The original transfer characteristics of the SO, without the L_1C_1 network, displayed a skirt selectivity of 15 dB/300 kHz. The

[2] The word "gain" or "sensitivity" is defined by (13) or $\overline{V}_o/\overline{V}_i$, but differs slightly from its standard usage. The output amplitude of the SO remains constant for varying input signal levels. The change of gain in (13) is due to $\overline{V}_i$ only.

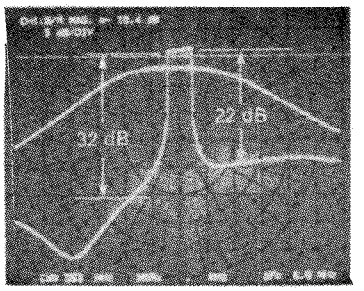

Fig. 9. Gain-synchronization curve of SO shown in Fig. 8 with L_1C_1 network. 560-MHz center frequency.

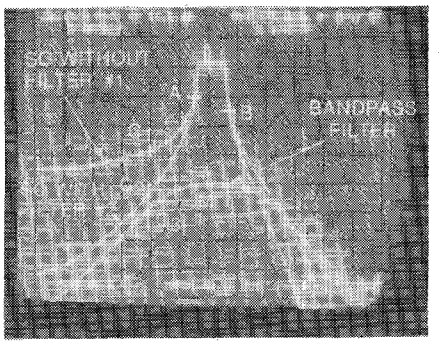

Fig. 10. Gain-synchronization curve of SO with input filter and 70-MHz center frequency.

incorporation of L_1C_1 increased the selectivity to 15 dB/40 kHz with 32 dB and 22 dB out-of-band rejection as shown in Fig. 9. Superimposed on the SO gain-synchronization curve is the transfer characteristics of a three-section 560-MHz bandpass filter. Fig. 10 illustrates a gain-synchronization curve of a standard 70-MHz SO, the transfer characteristics of a three-section 70-MHz bandpass filter, and the combined gain-synchronization curve with the bandpass filter connected to the input of the SO. The influence of the input filter illustrates the importance of the input coupling network on the regeneration process, where the latter increases the out-of-band attenuation of the SO faster than the attenuation provided by the input filter. We can observe the high internal gain of the SO is sufficient to compensate for filter losses within the lock-in range.

Fig. 11 illustrates the gain-synchronization curve of the 70-MHz SO with harmonic injection at 140 MHz. We notice the phase shift is ±45° due to the division process

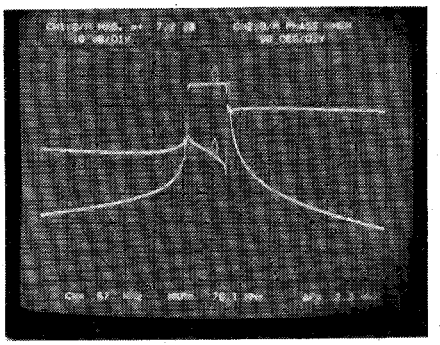

Fig. 11. Harmonic injection at 140 MHz into a 70-MHz SO.

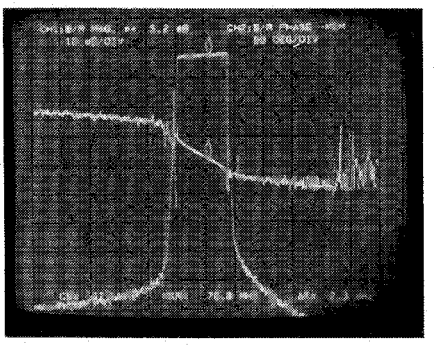

Fig. 12. The SO of Fig. 11 with a three-section 140-MHz filter connected to the input.

by the SO and the "gain-attenuation" level and skirt selectivity are dramatically increased with a gain scale of 10 dB/div. Fig. 12 demonstrates the gain-synchronization curve of the same SO with a 140-MHz filter connected to the input. We notice further enhancement of skirt selectivity and out-of-band attenuation. The former is approximately 24 dB/10 kHz in contrast with a three-section filter of 24-dB/3.6-MHz skirt selectivity. The performance enhancement with cascaded SO's will be described in the section on Carrier Recovery.

B. Frequency Division with SO's

SO's can divide by integers as well as rational integer numbers [20], such as 4, 1/4, and 3/2. Fig. 13 illustrates the injected waveform and the oscillator waveform in a division-by-1/4 process. We observe the synchronization occurs when the input waveform is at its maximum and the output waveform at it minimum. Fig. 14 depicts a division process by 3/2 where every third injected waveform synchronizes every second oscillator waveform. As the synchronization between the injected carrier and the oscillator waveform occurs at only one point in time, there cannot be false lock when SO's are employed in burst modem applications. Each division process by 2 reduces the phase shift between input and output of the SO by 90°.

C. Storage Time in SO's

Another interesting and useful feature of the SO is its capability to store or retain input frequency information. The degree of storage depends upon the input signal level.

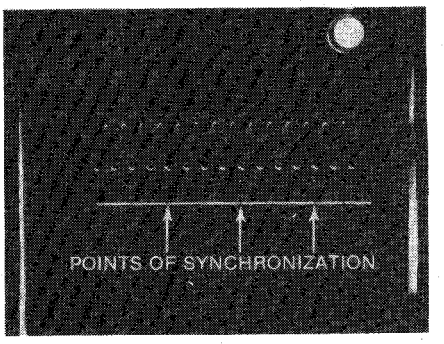

Fig. 13. Synchronization in a divide-by-1/4 process.

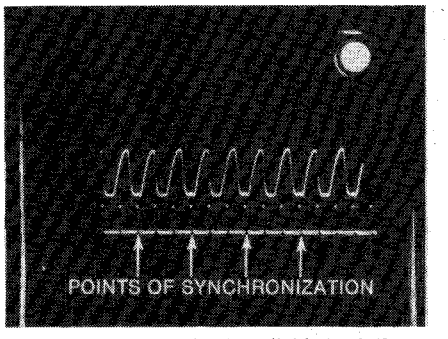

Fig. 14. Synchronization in a divide-by-3/2 process.

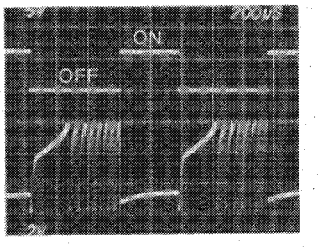

Fig. 15. Storage in an SO with −12-dBm signal drive.

This feature of the SO is especially useful in clock recovery networks [21] when the data consist of a time sequence of all "ones" or all "zeros" for an extended period of time, whereby no synchronization pulses are provided to the SO. During this period of time the SO continues to oscillate at the frequency or near the frequency of the original data transitions. Figs. 15 and 16 show the memory time of an SO driven by -12 and -3 dBm, respectively. During the positive pulses the injection frequency is applied to the SO, whereas during the negative pulses the SO is free-running. A phase detector detects the phase error between the injected carrier and the output of the SO and displays the error on a scope. When the SO is injected with the external carrier, the SO is synchronized and the phase detector supplies a dc output to the scope. In the absence of signal injection, the SO tries to return to its natural frequency and the difference of frequency appears on the scope. The time for the SO to return to its natural frequency is considered as the storage time.[3] While the SO tries to

[3] In general, clock recovery networks operate with signal-to-noise levels well above 0 dB and sufficient signal drive to utilize the inherent memory or storage in SO's.

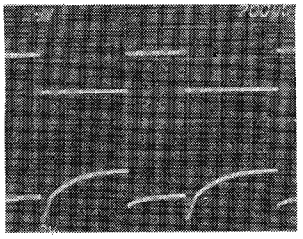

Fig. 16. Storage in an SO with −3-dBm signal drive.

return to its natural frequency, shortly after the injected carrier is turned off in Fig. 15, the phase detector output level remains at dc through the turn-off time in Fig. 16 indicating a higher storage time.

D. Acquisition Time in SO's

We can estimate the acquisition time of an SO which is synchronized by its natural frequency (i.e., low offset). In this case, (15) can be written as

$$\tau(1 \text{ percent}) \doteq \frac{1}{K} = \frac{2C_3\bar{V}_o}{G_{m1}\bar{V}_i} = \frac{1}{\pi(2\Delta f)} = \frac{1}{\pi\Delta f_o}. \quad (16)$$

For a 70-MHz SO with a 2-MHz tracking range we have the following measured parameters:

$$f_o = 70 \text{ MHz} \qquad G_{m1} = 100 \text{ mA/V} \qquad \bar{V}_i = 2 \text{ mV}$$
$$\Delta f_o = 2 \text{ MHz} \qquad C_3 = 8 \text{ pF} \qquad \bar{V}_o = 2 \text{ V}$$

which yields an acquisition time $\tau = 160$ ns in agreement with experimental results on SO's below 100 MHz. At higher frequencies the acquisition time becomes larger due to the input time constant of the SO and wiring/parasitic effects. The frequency offset affects the acquisition time when $\Delta\omega \to K$. In general, the maximum frequency offset in communication systems does not exceed ± 100 kHz, which justifies the approximation in (16).

E. SO's in the Nonfundamental Mode of Operation

We have discussed, in connection with Figs. 11 and 12, the performance of an SO with harmonic excitation. For example, a 70-MHz SO can be synchronized by 140, 210, 280 MHz, etc., and an output signal recovered through a bandpass filter. This output signal possesses superior signal-to-noise characteristics when compared with 70-MHz excitation, which is called the *fundamental-mode of operation*. The harmonic excitation or *nonfundamental mode of operation* is an important property of the SO and is enhanced by the nonlinear operation of the SO, which creates a high harmonic content in the output signal. For example, an SO which has a 130-MHz free-running frequency is synchronized by a 390-MHz carrier and the output is recovered at 390 MHz. The waveform of this specific SO is rich in the third harmonic (−36.2 dBm) as shown in Fig. 17. Experimental SO's with high third harmonics when injected with third harmonics have shown to have wide tracking range. Fig. 18 demonstrates the

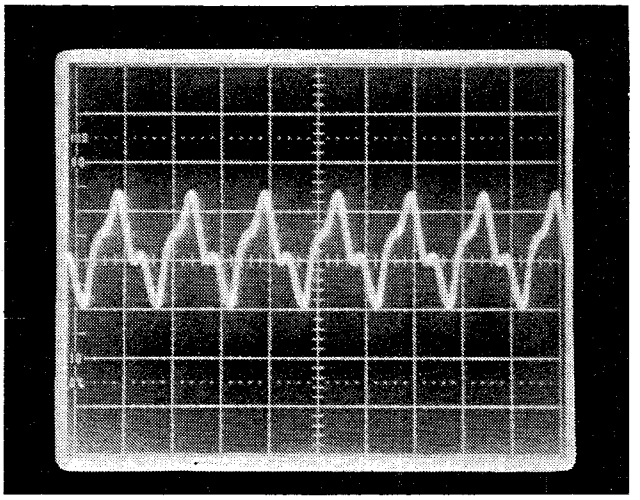

Fig. 17. High harmonic content in the SO's output waveform: 131 MHz (−26.3 dBm); 262 MHz (−45.1 dBm); 393 MHz (−36.2 dBm).

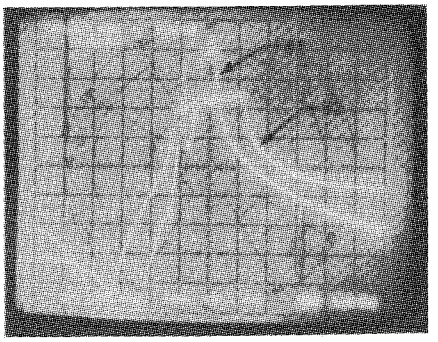

Fig. 18. Fundamental versus nonfundamental mode of operation: #1 — SO transfer function with fundamental (131-MHz) excitation; #2—SO transfer function with nonfundamental (393-MHz) excitation.

increase in tracking range for the harmonically pumped SO over the SO in the fundamental mode. The tracking range is increased by the order of the harmonic ($N = 3$) and the sensitivity is enhanced by the increased third harmonic content in the oscillator output signal. We should note that the analysis presented in this paper deals primarily with linear "pure" sinusoidal SO waveforms.

F. Filtering Properties of SO's

Due to the narrow resolution bandwidth the input thermal noise of the SO ($\bar{e}_f^2 = 4$ KTBR) is very low and thus the input sensitivity very high. It is interesting that the sensitivity (gain) increases as the input level reduces (see Fig. 7). This is why an SO can track signals as low as −100 dBm. The SO has two functional properties which determine noise rejection (filtering): the skirt selectivity of the tracking curve and the resolution bandwidth. The skirt selectivity defines the same functional properties as a linear filter is SOs operating in their fundamental mode. Steeper skirt selectivity means higher number of poles and thus better noise rejection [18], [19].

The SO has a resolution bandwidth similar to the operation of a spectrum analyzer. This is an important feature of an SO which does not exist in other tracking networks, such as phase-lock loops or Costas loops. In a phase-lock

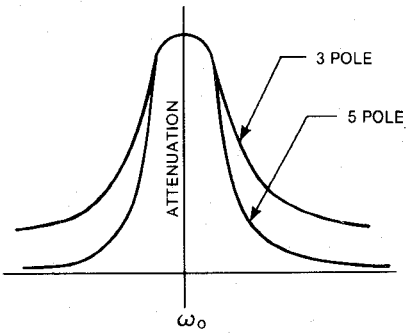

Fig. 19 Conventional filter transfer characteristics.

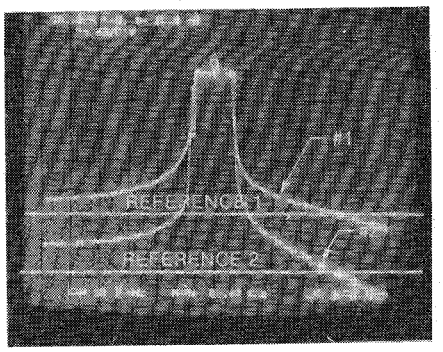

Fig. 20. Transfer characteristics of an SO with and without input filter.

loop when the loop filter bandwidth is defined, both the noise rejection and tracking range are fixed. They must be compromised in a given design. In a SO the tracking range and resolution bandwidth are independent of each other and can be optimized individually. The resolution bandwidth in an SO is a function of the internal regeneration process or Q-multiplication and can be less than 1 kHz. The external signal is incorporated in the regeneration process instantaneously. This is why an SO can track signals with -40-dB signal-to-noise ratio. The skirt selectivity of an SO can be improved by increasing the attenuation, not necessarily the gain. For example, Fig. 19 illustrates the transfer characteristics of two bandpass filters with three and five poles. The five-pole filter has steeper skirt selectivity and higher out-of band attenuation and, therefore, better noise-rejection properties. The bandpass gain level remains almost the same while the skirt selectivity increases in the five-pole filter. The transfer characteristics of four-terminal networks, whether linear or nonlinear, display the same functional properties. High skirt selectivity and low resolution bandwidth are the basic requirements for improved noise rejection. The SO's attenuation characteristics in the driven but unlocked region (see Fig. 3) are determined by the carrier injection level. Thus, two SO's which display the same relative transfer characteristics and identical skirt selectivities may have completely different noise rejection properties depending upon the variation in G_m's. From (13) and Fig. 3 we can write the out-of-band attenuation as

$$\text{attenuation (dB)} = -20 \log [2\Delta\omega/K]$$

$$= -20 \log [4C\bar{V}_o\Delta\omega/G_{m1}\bar{V}_i]. \quad (17)$$

Other factors remaining the same, the SO which has the lower G_mV_i product possesses the higher out-of-band rejection and steeper skirt selectivity. Fig. 20 illustrates two gain-synchronization curves for the same SO with (#2) and without (#1) an input filter to alter operating conditions. Thus, SO's require the specification of the carrier injection level V_i and the gain G_{m1} in order to assure uniform absolute transfer characteristics.

An SO exhibits high noise rejection while maintaining a wide tracking range. To illustrate the interesting properties of an SO we have performed noise measurements with the setup shown in Fig. 21. The carrier source is applied while

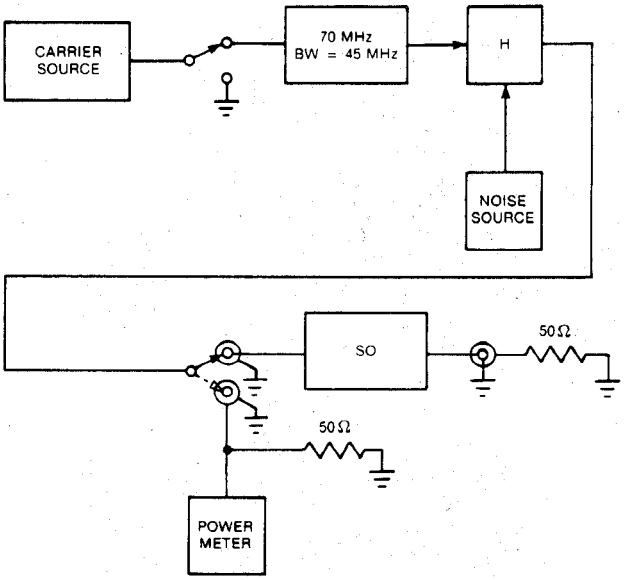

Fig. 21. Experimental determination of SO performance under noise injection.

the noise is inhibited and vice-versa to determine the carrier and noise power across the 50-Ω load. The carrier and noise sources are actuated and the output of the hybrid combiner H is applied to the SO. The 140-MHz bandpass filter with 45-MHz bandwidth serves as the reference for the injected carrier-to-noise level.

Fig. 22 shows the gain-synchronization curve of a 140-MHz SO with a -36-dBm carrier injection level while maintaining a 700-kHz tracking range. The carrier injection at the input of the SO is 4 mV. Fig. 23 shows the gain-synchronization of the same SO under a -11-dB carrier-to-noise power (same signal level). We observe the tracking range of the SO is reduced by approximately 50 kHz. The input and output waveforms of the SO under these noise conditions are illustrated in Fig. 24. The carrier-to-noise ratio at the output of the SO is 28 dB with an overall 39-dB improvement between input and output. In order to achieve the same improvement with a linear bandpass filter, the filter should have less than a 0.5-kHz bandwidth in contrast with a 650-kHz tracking range of the SO. Thus, the following conclusions may be drawn from these experiments: 1) the noise reduces (slightly) the tracking range; 2) the SO performs as a narrow bandpass filter for each frequency it tracks (resolution bandwidth);

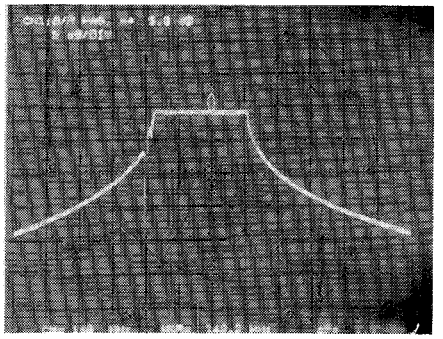

Fig. 22. 140-MHz SO with −36-dBm signal injection under low noise conditions.

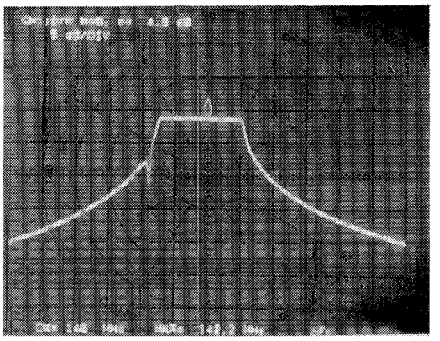

Fig. 23. 140-MHz SO with −36-dBm signal injection and −11-dB carrier-to-noise ratio.

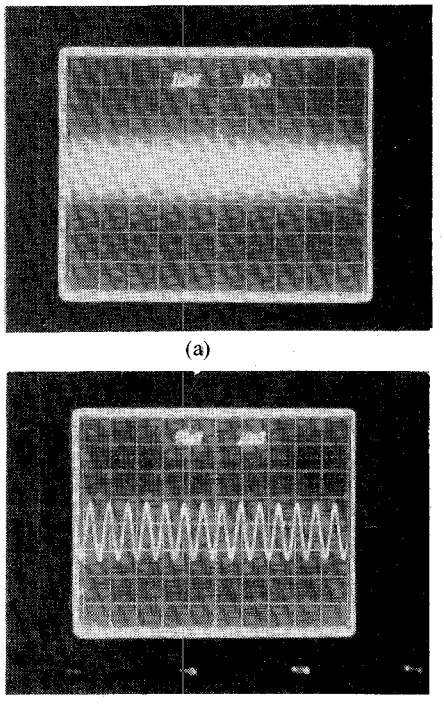

(a) (b)

Fig. 24. 140-MHz SO of Fig. 23. (a) Input signal. (b) Output signal.

3) the SO has a tracking range which is 1300 times its "effective" filtering noise bandwidth; and 4) as phase is a function of tracking range (see (14)), the phase error per frequency offset remains low. Thus, the SO is an adaptive wide-band tracking filter which has a very low resolution bandwidth and "locks" to the injected carrier within the tracking range with a high degree of noise rejection, while maintaining wide tracking range.

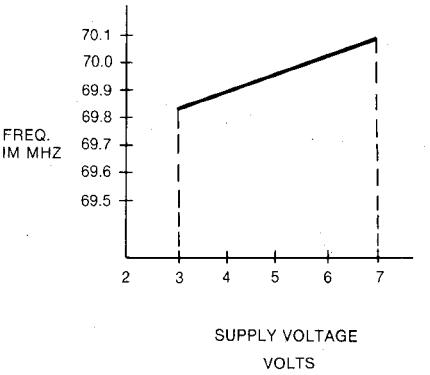

Fig. 25. Variation of SO's free-running frequency ω_0 as a function of supply voltage V_c.

Due to resolution bandwidth SO's have substantially higher noise rejection properties than phase-lock loops and Costas loops for a given tracking range. The SAW devices, however, which have higher Q than LC filters, still are far behind in noise rejection compared to SO's.

G. Temperature Compensation of an SO

The frequency stability of an SO is influenced by temperature and supply voltage fluctuations. In practice, we desire a stable free-running SO frequency under high temperature and a reduced phase error caused by frequency offsets. Fig. 25 illustrates the variation of the SO's free-running frequency as a function of supply voltage. Experimentally the free-running frequency of the SO decreases as the temperature increases. Thus, we can temperature compensate the SO by the insertion of a negative temperature coefficient resistor in series with the power supply. For example, a 560-MHz carrier recovery SO demonstrates a 30-ppm stability (16.8-kHz frequency drift) with a deterioration in the BER of only 0.3 dB between 15°C and 31°C when operated over a 24-h period.

H. Carrier Recovery with SO's [22]–[24]

SO's may be used as both carrier and clock recovery networks in QPSK modems. Carrier recovery requirements are more demanding than their clock recovery counterparts because of the low carrier-to-noise levels and the need for a wider tracking range. Thus, we will concentrate on the carrier recovery network as shown in Fig. 26. In this example, a 70-MHz IF is applied through a noise source to 4× frequency multiplier whose output is applied to a 280-MHz bandpass filter. The carrier-to-noise ratio at the output of the combiner is −3 dB. The output of the filter is amplified and applied to the 70-MHz SO. In the process of multiplying there is a −40-dBm power loss and a −18-dB degradation in the carrier-to-noise ratio. The 280-MHz filter bandwidth is maintained at 10 MHz so as not to disturb the acquisition time. The 70-MHz SO is injected with the 280-MHz carrier and the output recovered at 70 MHz. Figs. 11 and 12, previously discussed, illustrate the

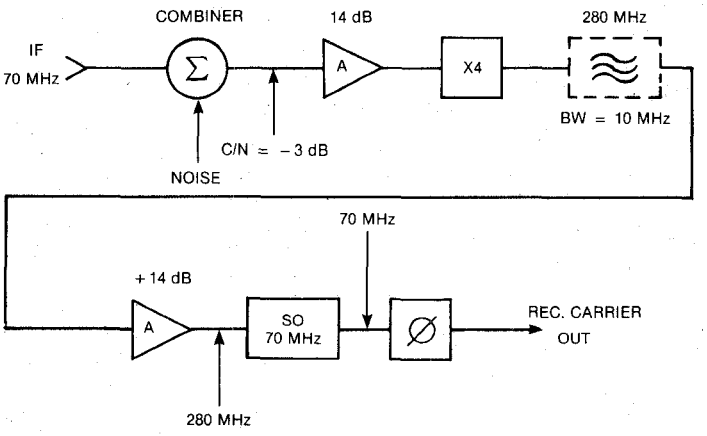

Fig. 26. SO carrier recovery network.

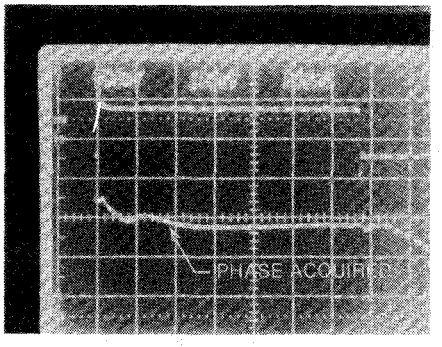

Fig. 27. Phase acquisition in the SO of Fig. 26.

gain synchronization curves of the SO carrier recovery network with and without the 280-MHz filter, respectively. The acquisition time of the carrier recovery network when the injected frequency is offset by 100 kHz from the free-running frequency is shown in Fig. 27. These results indicate acquisition occurs in less than 400 ns for the 100-kHz offset and less than 100 ns in the absence of frequency offset. Theoretical calculations based upon (15) for harmonic excitation ($N = 4$) indicate the acquisition time should be 160 ns, in excellent agreement with observations since experimental results include the delay time through the filter and the coupling networks. The input to the SO contains all the multiplication products and the filter characteristics of the SO are sufficient to remove these harmonics.

Clock and carrier recovery networks constructed with SO's have been tested in QPSK modems. The maximum deviation of the E_b/N_o ratio[4] (i.e., carrier-to-noise ratio at the output of the 70-MHz bandpass filter for a 60-Mbit/s data rate) from the theoretical value is 0.5 dB. The maximum deviation increases to 0.9 dB for a 150-kHz IF frequency offset. The unique synchronization properties of the SO (see Figs. 13 and 14) enable modem operation in the burst mode without false-lock. A test was carried out with no false-lock in the burst mode during a four-day operation period. The introduction of an interference signal, after acquisition to the synchronizing signal, does not disturb the original synchronization process. The SO remains locked to the synchronizing signal even though the interference signal has a comparable power level. The SO performance is illustrated in Figs. 28 and 29 for 60- and 120-Mbit/s modems. SO performance is *superior to standard PLL hardware*. The BER curve deviates only 0.2 dB from the hardwired case. The insignificant change in the BER performance due to frequency offsets and the improved performance over *the standard recovery networks*, using various versions of phase-lock loops, indicate the SO has a wider tracking range and higher noise rejection.

The 120-Mbit/s modems were tested in back-to-back operation and also while connected to the TDMA terminal. Tests were performed with a pseudorandom sequence of $2^{15} - 1$ bits. The carrier recovery network shown in Fig. 26 was used for the 120-Mbit/s modem. The 140-MHz SO was driven by 560 MHz. Due to high losses at 560 MHz (38 dB) on the standard PC board the signal-to-noise ratio was low and the tracking range was reduced to 300 kHz at $E_b/N_0 = 7$ dB. For wider tracking range two cascaded SO's were used to reduce the phase shift per unit frequency offset. The difference between the latter and the former BER results can be detected when the frequency offset exceeds ± 20 kHz. At lower frequency offsets the two BER results are the same as shown in Fig. 29. The unique word consists of two consecutive 12 bits. The preamble consists of 176 symbols, 48 of which are for carrier recovery and 128 for clock recovery. The guard time between bursts is variable and can be reduced to zero. The input to the receiver is $+2$ to -10 dBm. An AGC is used with a ± 6-dB dynamic range.

In certain applications, we may desire additional performance enhancement in SO synchronization networks. We have performed experiments with two cascaded SO's by the insertion of a 280-MHz SO between the 280-MHz filter and the 70-MHz SO in Fig. 26. In addition, we have isolated the two SO's with 3-dB pads. The gain and phase synchronization curves are shown in Fig. 30. The cascaded SO carrier recovery network displays over 1-MHz tracking range with an injected carrier to noise (before the $4\times$ frequency multiplier) of -3 dB, while its single SO coun-

[4] E_b/N_o (dB) = C/N (dB)—10 log (BW/BR), where C = carrier power, N = noise power, BW is the bandwidth of the IF filter, and BR the bit rate.

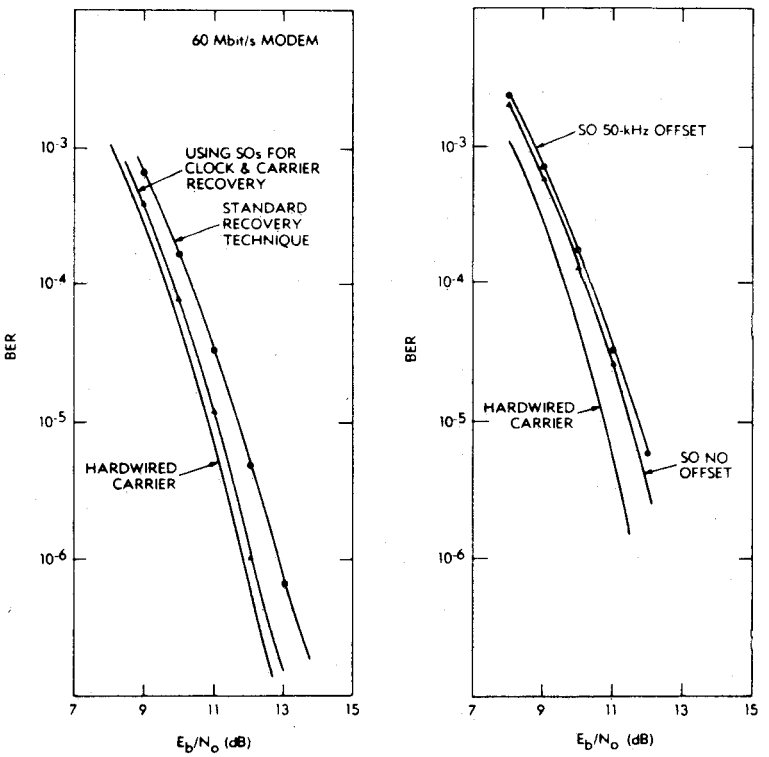

Fig. 28. BER performance of 60-Mbit/s modem.

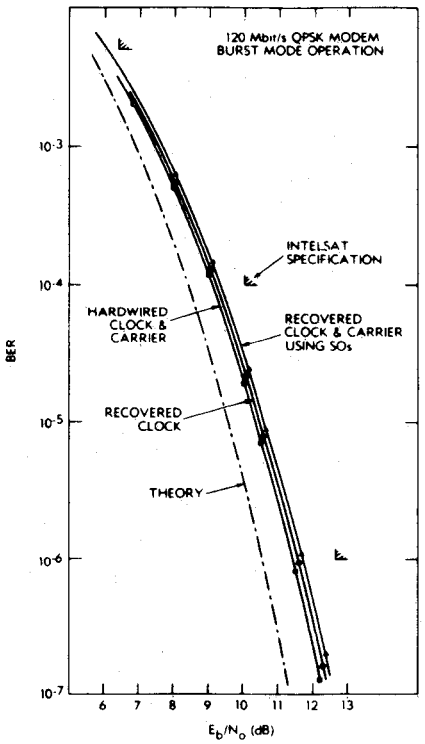

Fig. 29. BER performance for 120-Mbit/s modem.

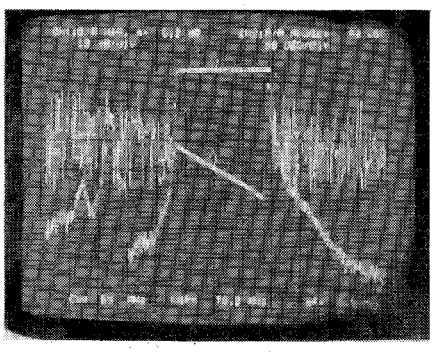

Fig. 30. Gain-phase characteristics for a cascaded carrier recovery network—SO_1 = 280 MHz, SO_2 = 70 MHz.

terpart, under identical conditions, displays a 150-kHz tracking range. In addition, the gain of the cascaded network is over 50 dB (see Fig. 30) as compared with 25 dB for the single SO network. The actual carrier-to-noise ratio at the input of the SO networks is −13 dB due to the −18-dB deterioration in the 4× multiplier and subsequent 8-dB improvement in the 280-MHz filter. In general, carrier recovery networks operate with carrier-to-noise ratios above 0 dB at the system input; therefore, cascaded operation of SO's in carrier recovery when the IF is under 140 MHz is usually not necessary.

IV. Conclusions

The synchronous oscillator (SO) is an important functional element for synchronization and tracking in communication systems. An SO is characterized by an adaptive instantaneous tracking bandwidth proportional to the magnitude of the input signal, while noise rejection is based mainly upon very narrow resolution bandwidth produced by the regeneration process of the oscillator. In the tracking range (i.e., the "lock-in" region) the output signal

amplitude remains constant and unaffected by variations in the input drive level; however, the output phase is modulated to synchronize and track the input signal even to power levels as low *as* -100 *dBm* while sustaining a 18-kHz tracking range. Thus, the SO performs like a narrow-band adaptive filter with an instantaneous tracking bandwidth, high skirt selectivity, and narrow resolution bandwidth for high noise rejection. Single SO carrier recovery networks have demonstrated improvement by 40 dB of the input signal-to-noise ratio, while maintaining a 800-kHz tracking range at input signal-to-noise level of -11 dB. Cascaded SO's under the same conditions have demonstrated a 60-dB improvement while extending the tracking range to 1.6 MHz. The acquisition time of the SO is inversely proportional to the tracking bandwidth ($2\Delta\omega = G_m\overline{V}_i/C\overline{V}_o$) for low-frequency offset. For example a 70-MHz SO can perform phase acquisition in less than 400 ns and track a 140-MHz carrier with an input signal-to-noise ratio of -40 dB while maintaining a 400-kHz tracking range. Extending the tracking range to 2 MHz in the same SO provides acquisition times less than 100 ns. The ability to achieve high-speed phase acquisition is an important feature in burst-modem applications. In addition to sensitivity, filtering (selectivity), wide tracking range, and fast acquisition, the SO possesses linear phase-shift characteristics for the useful tracking range which provides a *constant group delay*. The high internal gain of the SO reduces the steady-state phase error in synchronization to a low value ($\phi_{ss} \doteq \Delta\omega/K$) where $\Delta\omega$ is the frequency offset and K the injection constant defined by (14). An important aspect of SO's, especially in clock recovery networks, is an *inherent memory* (*storage time*) *corresponding to 20–25 bits* which may be adjusted so as not to deteriorate the acquisition time and BER. SO's may be used in applications other than carrier and clock recovery networks for modems. For example, SO's are excellent RF filters and integer (non-integer) frequency dividers/multipliers. In addition, SO's may be used as synchronization networks for minimum shift keying (MSK), phase-shift keying (PSK), and spread-spectrum communication systems. SO's can be used also in FM to improve selectivity and carrier-to-noise levels. (The BER results obtained on 60 and 120-Mbit/s QPSK modems indicate SO's can perform high-speed synchronization and tracking, especially in burst-mode operation, with performance near hard-wired transmission (0.4 dB from theory) without false locks and with long-term stability at elevated temperatures.)

This paper has described a new synchronization and tracking network, the *synchronous oscillator* (SO). We have discussed a particular application, namely, carrier and clock recovery in high-speed QPSK modems operating in the burst-mode; however, the useful properties of SO's extended well beyond the subject of this paper and impact applications where synchronization and tracking of signals embedded in noise are desired. The concepts presented in this paper can be realized together with support circuitry on a single integrated chip with *RC*-type continuous or switched capacitor filters.

ACKNOWLEDGMENT

The authors would like to express their appreciation to E. Fthenakis and D. Robinson for their encouragement and support in the application of SO's to advanced communication systems. In addition, we would like to thank J. Buzzelli and M. Soleimani for the BER measurements and T. Flamouropoulos for his contributions to nonlinear analysis and modeling. A special appreciation is due R. Adler and P. Runge for helpful discussions regarding the injection-type oscillators.

REFERENCES

[1] B. Van der Pol, "Forced oscillations in a circuit with nonlinear resistance," *Phil. Mag.*, vol. 3, p. 65, 1927.
[2] ——, "The nonlinear theory of electric oscillations," *Proc. IRE*, vol. 22, p. 1051, 1934.
[3] R. Adler, "A study of locking phenomena in oscillators," *Proc. IRE*, vol. 34, p. 351, 1946.
[4] K. Kurokawa, "Noise in synchronized oscillators," *IEEE Trans. Microwave Theory Tech.*, vol. MTT-16, p. 234, 1968.
[5] ——, "Injection locking of microwave solid-state oscillators," *Proc. IEEE*, vol. 61, p. 1386, 1973.
[6] R. V. Khoklov, "A method of analysis in the theory of sinusoidal oscillations," *IRE Trans. Circuit Theory*, vol. CTT-7, p. 390, 1960.
[7] N. Minorsky, *Nonlinear Oscillations*. Princeton, NJ: Van Nostrand, 1962, chs. 18–22.
[8] Hayashi, *Nonlinear Oscillations in Physical Systems*. New York: McGraw-Hill, 1964, chs. 5–7.
[9] E. Dewan, "Rhythms," *Science and Technology*, pp. 20–28, Jan. 1969.
[10] ——, "Harmonic entrainment of Van der Pol oscillations; Phase-locking and asynchronous quenching," *IEEE Trans. Automatic Control*, vol. AC-17, p. 655, 1972.
[11] P. Runge, "Phase-locked loops with signal injection for increased pull-in and reduced output phase jitter," *IEEE Trans. Commun.*, vol. COM-24, p. 636, 1976.
[12] V. Uzunoglu, "Carrier recovery networks for QPSK modems employing synchronous oscillators," U.S. Pat. 4 355 404, Oct. 19, 1982.
[13] V. Uzunoglu, "Synchronization and synchronous oscillators," in *Advances in Communications*, vol. 1. New York: Reidel, 1980, p. 437.
[14] ——, , "Phase-locked synchronous oscillators as carrier recovery networks," in *Proc. SCC-1983*, Ottawa, Canada, June 14–17, 1983.
[15] F. Gardner, *Phase Lock Techniques*. New York: Wiley, 1966, chs. 5–9.
[16] M. Armand, "On the output spectra of unlocked driven oscillators," *Proc. IEEE*, vol. 57, p. 798, 1969.
[17] T. Flamouropoulos, "An analysis of the nonlinear transconductance in a synchronous oscillator," M. S. thesis, Lehigh Univ., Bethlehem, PA, 1985.
[18] H. Bode, *Network Analysis and Feedback Amplifier Design*. Princeton, NJ: Van Nostrand, 1945.
[19] Kuo, *Network Analysis and Synthesis*. New York: Wiley, 1962.
[20] V. Uzunoglu, "Division by non-integer numbers using synchronous oscillators," U.S. Pat. 4 356 456, Oct. 26, 1982.
[21] V. Uzunoglu, "Universal clock recovery network for QPSK modems," U.S. Pat. 4 274 067, June 16, 1981.

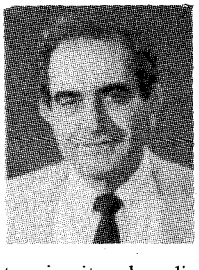

Vasil Uzunoglu (S'51–A'51–M'57) received the M.S.E.E. degree from the Missouri School of Mines and Metallurgy, Rolla, MO, in 1951.

During the course of his career he has worked at Bell Telephone Laboratories, Murray Hill, NJ, in semiconductor device characterization, Westinghouse, Baltimore, MD, in microelectronics research and development, and COMSAT, Clarksburg, MD, in the development of high-speed modems and adaptive equalizers. In the last 12 years he has developed the synchronous oscillator circuit and applied this concept to carrier and clock recovery networks in high-speed QPSK modems and various tracking networks. Currently,

he is with Fairchild Communications and Electronics Company in Germantown, MD, as Director of the Communications Laboratory, where he is responsible for the design and development of modems, adaptive equalizers, and voice processing systems. He is the holder of more than 30 U.S. Patents and is the author of the textbooks *Semiconductor Network Analysis and Design* and *Analysis and Design of Digital Systems*.

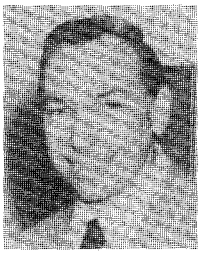

Marvin H. White (A'62–SM'71–F'74) was born in the Bronx, NY, on September 6, 1937. He received the A.S. degree in engineering from Henry Ford Community College, Dearborn, MI, in 1957, the B.S.E. degree in physics and mathematics and the M.S. degree in physics from the University of Michigan, Ann Arbor, in 1960 and 1961, respectively, and the Ph.D. degree in electrical engineering from Ohio State University, Columbus, in 1969.

During 1973–1976, he was the *Electron Device National Newsletter* Editor. In 1978, he was a Fulbright Visiting Professor in Microelectronics at Université Catholique de Louvain, Louvain-la-Neuve, Belgium. From 1976 to 1980, he served as Professor (part-time) at the University of Maryland, College Park. From 1961 to 1981, he was affiliated with the Westinghouse Electric Corporation, Advanced Technology Laboratories, Baltimore, MD, as an Advisory Engineer in the areas of electron devices and integrated circuits with 25 U.S. Patents awarded. He performed research and development silicon-diode camera tubes, electrooptical photodiode imaging arrays, MOS and CMOS transistors, bipolar and MOS LSI integrated circuits, low- and high-power microwave transistors, MNOS memory transistors, and CCD's for imaging, memory, and advanced signal processing. In 1981, he joined the faculty at Lehigh University, Bethlehem, PA, as Sherman Fairchild Professor of Electrical and Computer Engineering. He is involved in graduate education and microelectronics research with emphasis on solid-state device modeling and characterization for custom VLSI applications. In 1982, he served as the Electron Device National Guest Lecturer on modeling of small-geometry devices for VLSI.